
Research article

Thermal energy storage using phase-change material in evacuated-tubes solar collector

Akthem Mohi Al-Abdali* and Handri Ammari

Department of Mechanical Engineering, Mutah University, Mutah, Karak 61710, Jordan

* **Correspondence:** Email: akthemmoh9@gmail.com; Tel: +9647734641428.

Abstract: The use of phase change materials in solar thermal collectors improves their thermal performance significantly. In this paper, a comparative study is conducted systematically between two solar receivers. The first receiver contains paraffin wax, while the other does not. The goal was to find out to which degree paraffin wax can enhance the energy storage and thermal efficiency of evacuated tubes solar collectors. Measurements of water temperature and solar radiation were recorded on a few days during August of 2021. The experimental analysis depended on two stages. The first stage had a flow rate of 7 L/hr, and the second stage had no flow rate. A flow rate of 7 L/hr gave an efficiency of 47.7% of the first receiver with phase-change material, while the second conventional receiver had an efficiency rate of 40.6%. The thermal efficiency of the first receiver during the day at which no flow rate was applied was 41.6%, while the second one had an efficiency rate of 35.2%. The study's significant results indicated that using paraffin wax in solar evacuated tube water-in-glass thermal collectors can enhance their thermal energy storage by about 8.6% and efficiency by about 7%. Moreover, the results revealed that the solar thermal collector containing paraffin wax had an annual cost of 211 USD/year. At the same time, the receiver's yearly fuel cost was 45 USD. Compared to an electrical geyser, the annual cost reached 327 USD, with an annual fuel cost equaled 269 USD. The first receiver's payback period was 5.35 years.

Keywords: solar evacuated tube collector; thermal efficiency; thermal energy storage; paraffin wax

Abbreviations: \dot{Q}_u : The solar collector's useful thermal energy; \dot{m}_w : The water mass flow rate; AC_{Fuel} : Fuel's annual cost; $A_{Receiver}$: The storage tank's surface area; Cp_{PCM} : The paraffin wax's

specific heat; C_{p_w} : The water specific heat; E_{HW} : The overall thermal energy required to heat up the water; LH_{PCM} : The paraffin wax latent heat; OIC_{SC} : The solar collector's total initial cost; Q_{Loss} : The thermal energy lost from the water receiver; Q_{PCM} : The thermal energy stored in the paraffin wax; Q_i : The total energy received by the solar evacuated tube water-in-glass collector; Q_w : The thermal energy stored in water; $T_{PCM,avg}$: The paraffin wax mean temperature of four thermocouples temperature values; $T_{w,in}$: The inlet water temperature to the solar collector; $T_{w,out}$: The outlet water temperature from the solar thermal collector; U_t : The overall uncertainty; f_{L-PCM} : The paraffin wax fraction converted into liquid phase; k_{ins} : The insulation's thermal conductivity; m_{PCM} : The paraffin wax's mass; m_w : The water mass; n_{Days} : The days' number on which hot water is demanded; AS : The annual savings attained via using solar collector; CE : The electricity cost; CRF : Capital recovery factor; $I(t)$: The solar irradiation; IC : The overall system's initial cost; N : The number of times the variables are measured; $O\&MC$: Yearly cost of operations and maintenance; P : The solar collector's present value; PBP : The payback period; SFF : Sinking funding factor; SV : The overall system's salvage value; α : The solar collector's absorptivity; ε_r : The random errors in the experimental work; ε_s : The systematic errors in the experimental work; η_{coil} : The electric heater's (geyser's) efficiency; η_{SC} : The solar thermal collector's efficiency; η_d : The solar collector's thermal efficiency during a day; $\bar{\varphi}$: The mean measured amount; τ : The solar collector's glass transmissivity

1. Introduction

The employment of numerous solar thermal heaters has been developing in the last decades. They provide a high-reliability rate, low maintenance cost, and useful energy savings to the electrical bill for various industrial and commercial applications. In addition, solar thermal collectors are well-known for their functional potential in saving carbon and greenhouse gas (GHG) emissions, causing no negative impact on the environment. Solar thermal heating relies on accessible solar radiation to offer thermal energy. They are a good alternative energy resource to supply power as a replacement to several fossil fuel resources. Scholars estimated that crude oil is going to deplete before 2050 [1]. Research and development works are applied to several solar thermal collectors, resulting in innovative modifications and improved thermal efficiency and performance. Solar collectors can be categorized into five principal types. These types are: (i) evacuated-tube solar collectors, (ii) concentrated solar collectors, (iii) flat-plate thermal collectors, (iv) Photovoltaic (PV)-based solar collectors, and (v) asphalt thermal collectors [2]. Solar evacuated tube collectors are more efficient than other solar thermal collectors. They use vacuum to reduce heat loss from solar evacuated tube collectors. Scholars classified evacuated tube solar thermal collectors into three main categories. These include (1) water-in glass evacuated-tube collectors, (2) heat pipe evacuated tube solar thermal collectors, and (3) U-tube thermal evacuated tube collectors [3]. This study investigates the performance of the water-in-glass evacuated tube solar collector, in which a comparative analysis is conducted for two water-in-glass solar thermal evacuated tube collectors. The first receiver has paraffin wax, while the other one does not. The use of smart solar thermal collectors integrating phase change materials (PCM) is vital. They can store thermal energy for longer periods and offer it at night or cloudy days. Abd-Elhady and his colleagues [4] reported that evacuated tube solar thermal collectors have an efficiency of around 49% to 57%. Further, utilizing PCM can accomplish significant improvements in the efficiency of evacuated tube solar thermal collectors. In this context, PCM can solve the intermittency issue of solar radiation. It can offer a functional solution to the winter conditions at which no sufficient solar radiation

is available. When solar radiation is accessible, solar thermal collectors can gather energy and store it in the receiver. PCM can boost the amount of thermal energy and provide it later when limited sun radiation is available. Another contribution of using PCM is their critical role in improving the solar thermal collector's reliability. It can save a large budget spent on the use of electrical geysers. A study conducted by Venkatacha [5] in which they have conducted a systematic review of major key characteristics of PCM and its key role in improving the potential of energy storage for different solar thermal collectors. Results of their systematic review revealed that using PCM in thermal energy storage can considerably increase the potential of thermal energy storage to store high quantity of thermal energy for longer time, which can help increase the economic feasibility of the whole system. A study conducted by Benchara [6] reviewed several publications and articles that discuss the significance and key role of integrating PCM in thermal energy storage. The results of their extensive literature review revealed that the use of PCM in thermal energy storage is highly effective and beneficial in increasing the rate of thermal energy and increase the duration of thermal energy storage. In addition, their results revealed that using PCM can achieve higher economic feasibility of the solar thermal collector and increase their reliability in providing hot water. A study conducted by Reddy [7] classified major contributions and key advantages of using PCM in thermal energy storage for solar water collectors. They conducted an experimental investigation, through which they developed a thermal energy storage system that uses PCM (including paraffin and stearic acid) for saving thermal energy from solar thermal collectors. Results of their experimental analysis revealed that using PCM in thermal energy storage can significantly increase the quantity of thermal energy generated from solar thermal collectors in very small area. Moreover, researchers found that using PCM (including paraffin and stearic acid) can lower energy losses and is more economically feasible, with no impact on the amount of thermal energy that is stored. In addition, the charging and discharging time is effective using PCM. A study conducted by Lin [8] to assess the major contribution of paraffin wax in increasing the performance of solar thermal system. They conducted a numerical analysis for investigating the performance of a solar thermal system after adding paraffin wax. Their results revealed that using paraffin wax in the solar thermal system has significantly increased the energy storage capacity of the system and increased its overall thermal efficiency.

The study conducted by Sadeghi and colleagues [9] aimed at a modified evacuated tube solar collector (METSC) with a bypass pipe utilizing copper oxide/distilled water ($\text{Cu}_2\text{O}/\text{DW}$) nanofluid experiments. The results demonstrated that the METSC performance was mostly impacted by the tank volume alteration. Moreover, using the $\text{Cu}_2\text{O}/\text{DW}$ nanofluid enhances the daily energy efficiency of METSC by up to 4%. While another study conducted by Chung-Yu Yeh and his co-worker [10] designed a solar thermal collector integrated with storage PCM. The salt hydrate-based composite PCM, with the sodium acetate trihydrate (SAT), was used to create a shape stabilized PCM of low leakage and high thermal conductivity.

In another study, Sadeghi and his co-worker [9] used copper-oxide nanofluid in a back-pipe vacuum tube solar collector accompanied by data mining techniques. This modification led to decreasing heat losses and improving heat transfer rate by 42% and 10%; respectively, and an optimum aspect ratio of the collector was obtained. Also, Sadeghi [9] worked on thermal energy storage development, materials, design, and integration challenges. He addressed in a multi-scale fashion from the component level to the system level to provide a broader perspective of this field of science.

A study by Shoeibi and colleagues [11] mentioned the use of nano-enhanced phase change materials in solar energy applications, where they indicated that the addition of nano-material to phase-

changing materials facilitates the charging and unloading processes of heat storage units due to the increased thermal conductivities and low melting points. In another study by Shoeibi et al. [11] on the effects of the nano-enhanced and nano-coated phase change material on the performance of the solar snapshots, the results indicated that the productivity of the solar snapshot improved by 55.8% and 49.5% using the nano-enhanced PCM CuO and Al₂O₃ at a concentration of 0.3% by weight and CuO nano-coated, respectively. In addition, the added nanoparticles of CuO and Al₂O₃ at 0.1 wt% reduced the melting point by 2.1 °C and 1.8 °C, respectively. The per liter price of solar droppers were \$0.1/L and \$0.104/L using CuO and Al₂O₃ nano-enhanced PCM at 0.3 wt% concentration and nano-coated, respectively. Moreover, nano-coating increased the rate of water production from solar energy by about 5.7%.

This study is carried out to investigate the contribution role and significant benefits when paraffin wax (a type of PCM) is integrated into evacuated water-in-glass solar collector that are commonly used in the region under regional climate conditions. It makes a comparative analysis between two water-in-glass solar collectors, one that includes the paraffin wax, while the other does not. The study also conducted an economic analysis to assess the potential of incorporating paraffin wax in solar evacuated tube collectors. The study depends on assessing the thermal energy stored and thermal efficiency for comparison purposes between the two solar evacuated tube collectors.

2. Experimental procedure and setup

In this research, comparative and experimental analyses are conducted by assessing the solar evacuated tube water-in-glass collector's performance when paraffin wax is integrated into the system. Measurements are taken in two stages. Stage one has a flow rate of 7 L/hr, while the second stage has no flow rate. In addition, this study conducts an economic analysis by comparing the profitability of solar evacuated tube collector with an electric geyser.

2.1. Experimental setup

In this research, the parts of two similar evacuated tube water-in-glass collectors were manufactured and assembled in Mutah University engineering workshop and a solar energy factory. Each absorber is comprised of eight evacuated tubes. The outer diameter of these tubes is 58 mm, while the inner diameter is 43 mm. Their overall length is 180 cm. The tube's glass transmissivity equals 0.92. The system includes two receiver tanks, with each is connected to one absorber. The first receiver (A) contains paraffin wax, while the other receiver (B) does not. In addition, a cold-water tank with a capacity of 1,000 liters was prepared to provide both receivers with cold water, with an external tank was used to refill the cold-water tank when needed. The system is shown in Figure 1. Figure 2 presents a schematic of the whole system incorporating the two models. Figure 3 shows a cross-section of the storage tank and the location of the PCM container, which is located in the middle of the tank (A). Tank (B), contains a plastic rod of the same diameter and length at its center as that of the inner cylinder having the phase-changing material in receiver tank (A) to ensure the same amount of water in both tanks in order to compare them and find out the effect of the heat energy stored by the phase-changing material on the efficiency and performance of the solar heater. The experiment was carried out in two stages, as mentioned above; one with a flow rate of heated water of 7 L/h for both receiver tanks, and the other with no flow rate in both tanks.

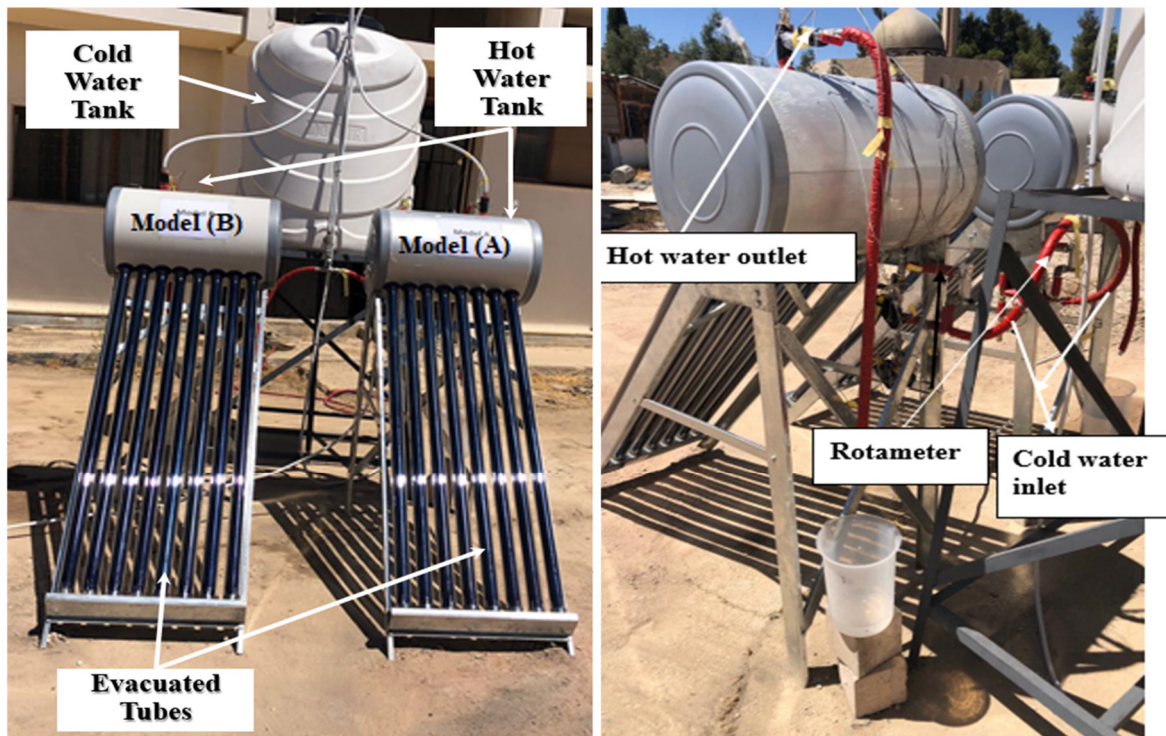


Figure 1. An experimental setup configuration of the two receivers; (A) contains paraffin wax, and (B) does not contain it.

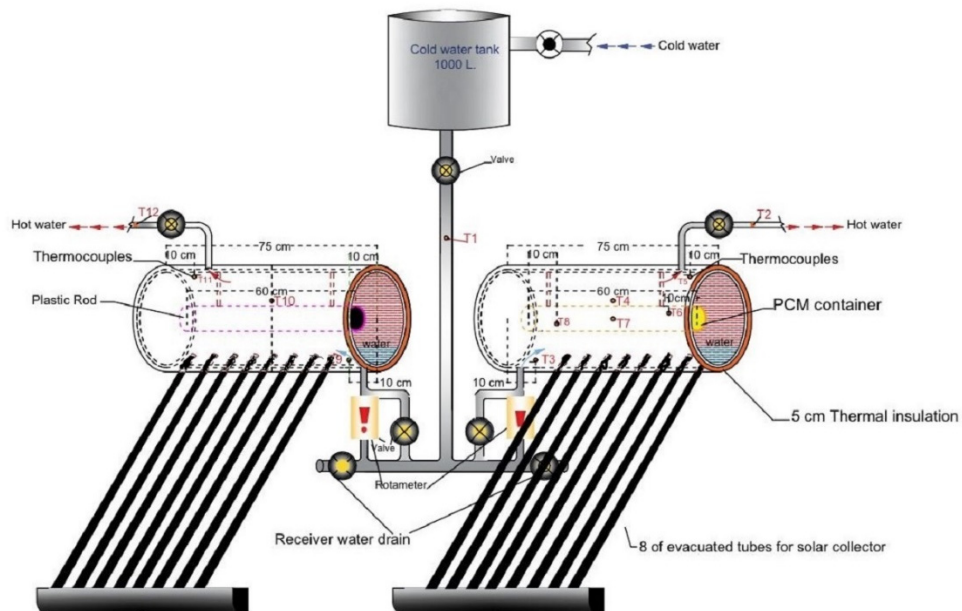


Figure 2. Schematic of the whole system with model (A) on the right, and (B) on the left.

A data logger is installed in models (A) and (B) to measure the temperature at different locations, see Figure 3.

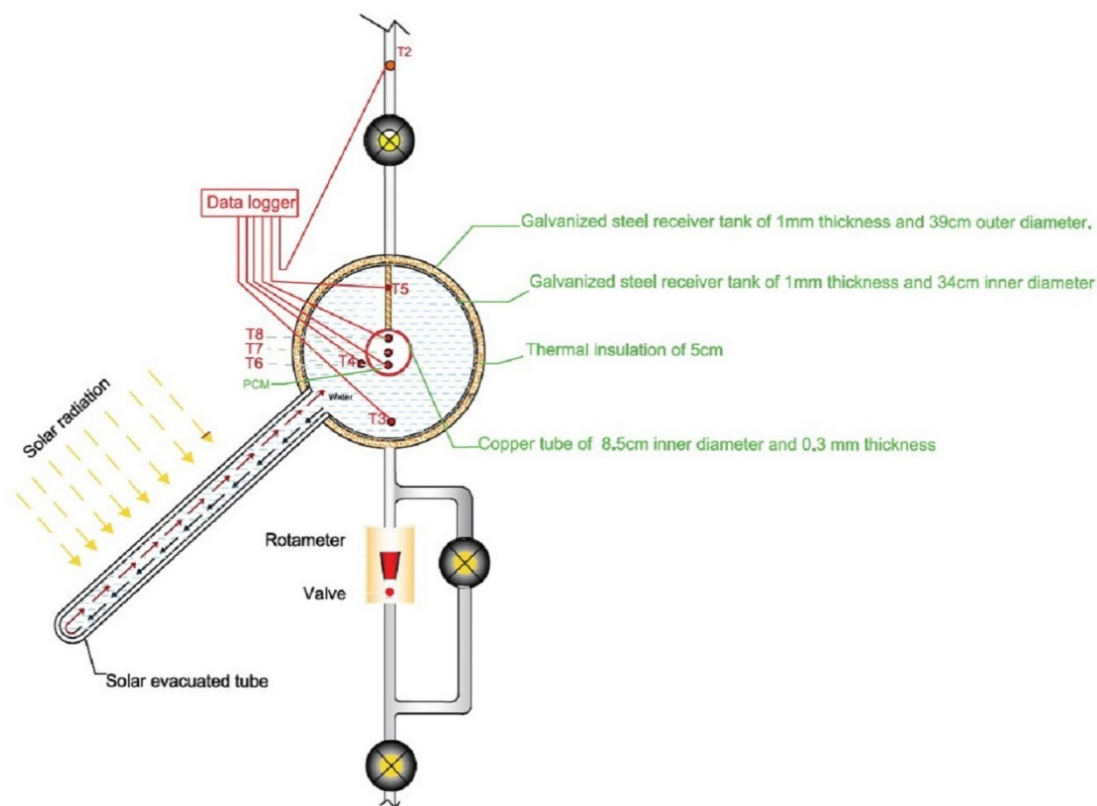


Figure 3. Schematic diagram of data logger installed in the water cycle of the model (A).

2.2. Selection of paraffin wax

Paraffin is a mixture of hydrocarbons, so it does not have a draconian melting point like the pure compound. The melting point of paraffin wax is the temperature at which the paraffin sample cools and melts under certain conditions. All wax products must be temperature resistant to paraffin, i.e., they must not melt or soften at a specific temperature. Depending on the conditions of usage, the region and season of use, and the environment in which they are employed, paraffin waxes must have a variety of melting points. The key element determining the melting point of paraffin is the oil content. The melting point of paraffin wax is also influenced by the oil content. The melting point of paraffin wax decreases as the amount of oil in it increases [12]. Paraffin wax has the ability to store heat as latent heat energy that can be used in heating processes. Therefore, the selection of the wax sample depends on the degree of melting and the latent thermal energy, and in order to obtain a complete melting of the wax sample, the wax sample is chosen within the average temperature of the medium in which it is placed and in order to make maximum use of thermal storage in water heating. In our experiment, the operating temperature range was between (50–80 °C). Two specimens of PCM were chosen. The specimens are set for testing and evaluating their characteristics in the Laboratories of the Royal Scientific Society (RSS). Specimen (A) is a paraffin wax imported from China. Specimen (B) is a paraffin wax imported from India.

The RSS testing results as indicated in Table 1 affirmed that the Chinese paraffin wax specimen (A) has two melting points. The area (1, or 2) represents the latent thermal energy. The results also showed that the Chinese paraffin wax specimen (A) is more suitable and thermally functional compared to the Indian paraffin wax in terms of efficiency and thermal energy stored in our solar system. RSS results indicated a paraffin wax latent heat of 189.8 kJ/kg for the Chinese specimen. For specimen (B), the latent heat was lower (165.4 kJ/kg).

Table 1. The RSS testing results for samples (A)& (B).

Samples	Melting Temperature T_{m1}	Melting Temperature T_{m2}	Area (1)	Area (2)	Solid Density 23 °C
Sample (A)	38.4 °C	59.4 °C	41.72 J/g	148.12 J/g	0.83 g/cm ³
Sample (B)	68.8 °C	—	165.40 J/g	—	—
Sample from literature (1)	33.0 °C	54.9 °C	17.55 J/g	158.83 J/g	0.79–0.94 g/cm ³

The RSS results of both specimens are compared to those of [12,13]. The characteristics are remarkably approximate to the paraffin wax data collected by them. Their results showed that the paraffin wax latent heat equaled 190 kJ/kg, with a specific heat of 2.15 kJ/kg.K in liquid form, its melting point was 59.9 °C, and its solid phase density is 910 kg/m³.

A mass of 2.8 kilograms of paraffin wax is used in the experiment, based on the volume of the cylinder in which the paraffin wax was placed. Figure 4 illustrates the melting process and preparation phase of paraffin wax during integration into the inner cylinder in the receiver tank (A).



Figure 4. Preparation and melting process of paraffin wax.

2.3. Experimental procedure

Several measurements instruments were used to collect data related to temperature and solar irradiation. Twelve thermocouples in all were used, with seven installed in receiver tank (A) which contained paraffin wax (see Figure 3). Four thermocouples were utilized in the other receiver. The last thermocouple was installed at the common inlet water pipe that provided inlet water for the two

receivers. In addition, data loggers were installed in both receivers to measure the temperature values at several locations. The data logger used in this research is made by (CEM), having a model number of (DT-172TK). Further, a rotameter was used to measure and control the water flow rate into the two receivers. The rotameter used in this research is made by “Dwyer Company” having a model RMC-SSV-10. The rotameters controlled the exact flow rate into each receiver and an external water tank was used to replenish the cold-water tank’s level. A solar power meter is utilized to assess the solar radiation potential and intensity. The solar power meter used in this research is made by (CEM, having a model of [DT-1307]). The experiments were conducted for a few days during August 2021.

3. Performance analysis

The experimental analysis is performed using the relationships in section 3.1 to find the efficiency and economic feasibility of integrating paraffin wax into the solar evacuated tube collector.

3.1. Theory and mathematical modelling

To analyze the efficiency and thermal energy stored in the receiver some formulas are used. The total useful energy stored in the solar collector, Q_{tu} , is evaluated by:

$$Q_{tu} = Q_w + Q_{PCM} - Q_{Loss} \quad (1)$$

where Q_w is the thermal energy stored in water (in kJ), while Q_{PCM} is the thermal energy stored in the paraffin wax. Q_{Loss} is the thermal energy lost from the receiver containing the water, to compute the thermal energy stored in water, the following expression is utilized [14,15]:

$$Q_w = m_w C_{p_w} (T_{w,out} - T_{w,in}) \quad (2)$$

where m_w presents the mass of water computed by finding the multiplication of the water density at high temperature values (990 kg/m³ is the water density from 60 to 80 °C [16] with the hot water storage tank volume. C_{p_w} presents the water specific heat of 4.186 kJ/kg.K. However, it will become equal to 4.22 kJ/kg.K at temperature values from 55 °C to 75 °C. $T_{w,out}$ presents the outlet water temperature from the solar thermal collector. It is larger than the inlet water temperature to the solar collector of 25 °C, $T_{w,in}$. In addition, Q_{PCM} is computed using the expression:

$$Q_{PCM} = m_{PCM} C_{p_{PCM}} (T_{PCM,avg} - T_{PCM,in}) + f_{L-PCM} \times m_{PCM} \times LH_{PCM} \quad (3)$$

where m_{PCM} presents the paraffin wax’s mass of 2.8 kg. $C_{p_{PCM}}$ Presents paraffin wax’s specific heat (2.15 kJ/kg.K in liquid phase) [11], while $T_{PCM,avg}$ presents the paraffin wax mean temperature of four thermocouples temperature values. Further, f_{L-PCM} is the paraffin wax fraction converted into liquid phase. It equals to 1 when it is totally in liquid phase. In contrast, it equals to zero when it is in solid phase. LH_{PCM} presents the paraffin wax latent heat. Q_{Loss} can be calculated through the expression:

$$Q_{Loss} = k_{ins} A_{Receiver} \frac{(T_{w,avg} - T_{Amb})}{t_{ins}} \quad (4)$$

where k_{ins} presents the insulation's thermal conductivity. The insulation used in the receivers is polyurethane foam. Its thickness is 5 cm. The thermal conductivity of the polyurethane foam is 0.039 W/m. K [15]. $A_{Receiver}$ presents the storage tank's surface area through which convection and conduction of hot water's energy is transferred to the ambient outside the system. $A_{Receiver}$ value equals 1.392 m². Mathematical modeling is conducted to compute the solar thermal collector's efficiency, η_{SC} , for the two receiver tanks; with the integration of paraffin wax and without. η_{SC} is computed via the expression [13,15]:

$$\eta_{SC} = \frac{Q_u}{Q_i} \times 100\% \quad (5)$$

where Q_i is the total energy received by the solar evacuated tube water-in-glass collector, Q_i is estimated via the equation:

$$Q_i = A_{SC} \times I_T \times \alpha \times \tau \quad (6)$$

where A_{SC} is the overall solar collector's area subjected to direct irradiation, I_T is the total global irradiation on the solar collector's tilted surface. α is the absorptivity of the solar collector. τ presents the solar collector's glass transmissivity. In addition, the solar collector's useful thermal energy, \dot{Q}_u , is computed using the following formula. Not that water flow rate is applied.

$$\dot{Q}_u = \dot{m}_w C_p (T_{w,out} - T_{w,in}) \quad (7)$$

where \dot{m}_w presents the water mass flow rate (kg/s). The solar collector's thermal efficiency during a day, η_d , can be calculated via the equation:

$$\eta_d = \frac{\sum \dot{Q}_u}{\sum I(t) \times A_c \times \tau} \quad (8)$$

where $I(t)$ presents the solar irradiation, and τ is the glass's transmissivity. To calculate the hourly efficiency, the following formula is used:

$$\eta_H = \frac{\dot{Q}_{u,i}}{I_{t,i} \times A_c \times \tau} \quad (9)$$

where i is the hour.

3.2. Economic feasibility

To determine the solar collector's profitability when paraffin wax is integrated, the following formula can be exploited. The system's annual cost is computed through the equation:

$$AC_{Sys} = AC_{Fuel} - SFF \times SV + IC \times CRF + O\&MC \quad (10)$$

where AC_{Fuel} is the fuel's annual cost, SFF is the sinking funding factor, SV is the overall system's salvage value, IC is the overall system's initial cost, CRF is the capital recovery factor, and $O\&MC$ is the yearly cost of operations and maintenance. AC_{Fuel} is computed through the equation:

$$AC_{Fuel} = \frac{n_{Days} \times E_{HW} \times CE}{\eta_{coil}} \quad (11)$$

where n_{Days} presents the day's number on which hot water is demanded. Further, E_{HW} presents the overall thermal energy required to heat up the water. CE presents the electricity cost. η_{Coil} presents the electric heater's (geyser's) efficiency. SFF is calculated using the expression:

$$SFF = \frac{i}{[(1+i)^N - 1]} \quad (12)$$

where N presents the overall system's lifetime. At the same time, CRF is evaluated using the equation:

$$CRF = \frac{(1+i)^N \times i}{[(1+i)^N - 1]} \quad (13)$$

where i present the interest rate value. The solar collector's annual cost, A_{SC} , is evaluated through the equation [13]:

$$A_{SC} = P \times \frac{(1+i)^N \times i}{[(1+i)^N - 1]} \quad (14)$$

where P presents the solar collector's present value. The payback period, PBP , of recovering the solar collector's purchasing cost is evaluated via the equation [16]:

$$PBP = \frac{OIC_{SC}}{AS} \quad (15)$$

where OIC_{SC} is the solar collector's total initial cost, AS is the annual savings attained via the use of the solar collector.

3.3. Uncertainty analysis

Uncertainty is highly beneficial to determine the sources of errors that occurred during the experiment. The errors take place because of faults in making experimental measurements, or faults because of errors in the same devices used [17]. Eq (16) is used to analyze the uncertainty in the experimental work [18]:

$$U_t = \sqrt{\varepsilon_s^2 + \varepsilon_r^2} \quad (16)$$

where U_t is the overall uncertainty, ε_s is the systematic errors in the experimental work, ε_r is the random errors in the experimental work. ε_s is computed through the expression:

$$\varepsilon_s = \sqrt{\sum_{i=1}^n \varepsilon_{s,i}^2} \quad (17)$$

In addition, ε_r is computed via the equation:

$$\varepsilon_r = \sqrt{\sum_{i=1}^n \varepsilon_{r,i}^2} \quad (18)$$

where n is the errors source number, and $\varepsilon_{r,i}$ is given by the relation:

$$\varepsilon_r = \sqrt{\frac{\sum_{i=1}^n (\varphi_i - \bar{\varphi})^2}{N(N-1)}} \quad (19)$$

where N is the number of times the variables are measured. Whilst $\bar{\varphi}$ is the mean measured amount. In this research, the uncertainty amounts of electrical devices, used for measurements, are determined using the datasheet in appendix (B). Table 2 presents the uncertainty values of the electrical devices used in measuring and assessing the research parameters.

Table 2. Uncertainty of the devices used in this study.

Device	Measurement Parameters	Uncertainty Value	Uncertainty (%)	Notes
Thermocouple (TC-K2-TC-J2)	Water inside the receiver temperature, and paraffin wax temperature	± 0.013 °C	$\pm 0.5\%$	K-Type Thermocouple
Rotameter	Water flow rate	± 0.075	$\pm 4\%$	RMB-SSV Model
Solar power meter	Solar radiation	± 10 W/m ²	$\pm 1\%$	Range: 1 to 2000 W/m ²

In order to know the uncertainty of the readings of the experiment with regard to the readings of solar radiation, the readings measured by the device were compared with the readings of the Prince Faisal Center for Research and Energy, which is located near the site of the experimental setup and for the same day of the experiment. The results were very close to each other.

As for the Thermocouples, they were estimated using the equations above, and the ratio was within (0.43%).

4. Results and discussions

Results obtained from the experimental analysis of the two receivers provided data on thermal energy and thermal efficiency. The energy analysis is executed depending on the theory and mathematical model of this work. The following paragraphs indicate the thermal energy and efficiency results of the measurements recorded during the three days of testing.

4.1. Energy analysis of stage (1)—flow rate of 7 L/hr

Stage (1) is conducted on August 20, 2021. Figure 5 illustrates the solar irradiation and ambient temperature on August 20, 2021.

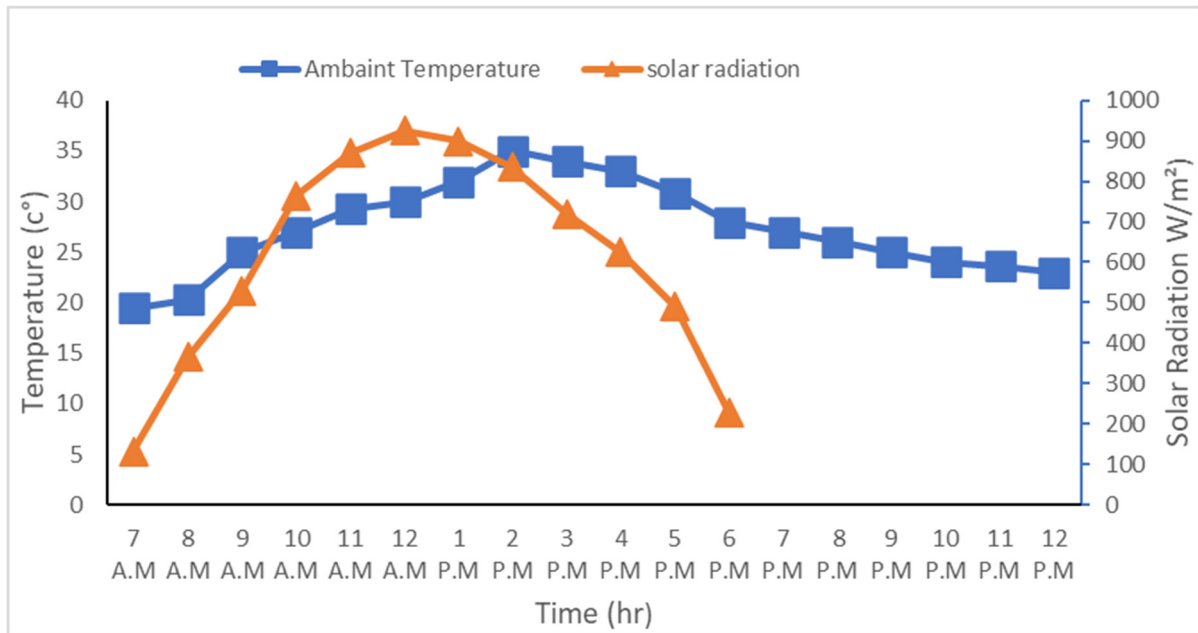


Figure 5. The solar irradiation and ambient temperature on August 20, 2021.

It is inferred from Figure 5 that the solar radiation increased from 7:00 A.M. with a value of 150 W/m² until noon. At noon the solar radiation is around 900 W/m². In addition, it is inferred from Figure 5 that the range of ambient temperature is between approximately 20 and 35 °C. The maximum radiation was at noon. In the afternoon, and after the earth's surface it was considerably heated up and stored thermal energy, it started to emit heat to the ambient causing a rise in the ambient temperature to about 35 °C at 2:00 P.M.

A comparative analysis is conducted between receivers (A) and (B). Figure 6 shows the thermal energy stored in watt-hour in the solar receiver's tanks (A) and (B).

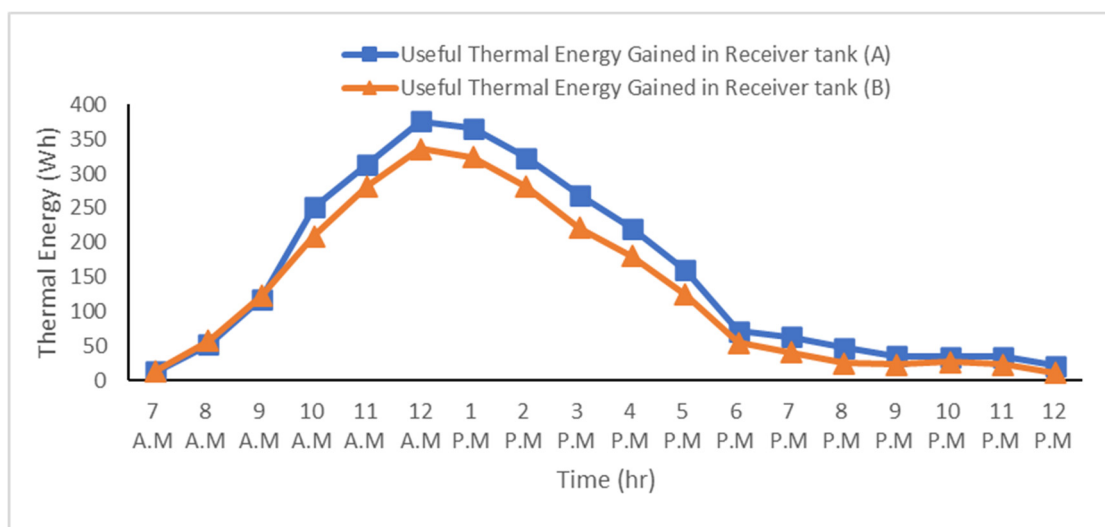


Figure 6. Profiles of receiver's tanks' useful thermal energy variation with time with a water flow rate of 7 L/hr.

It is concluded from Figure 6 that the thermal energy stored in receivers (A) and (B) increases with time starting from 7:00 A.M. The maximum value of the thermal energy is reached at a value close to 330 and 380 Wh for receivers (A) and (B), respectively. Also, it is observed that the useful thermal energy stored in the receiver (A) is higher than that of receiver (B) by about 8.6% at noon and about 30% at early night. Before noon, paraffin wax goes through the heating phase at which it absorbs thermal energy from water. The experimental data are also analyzed for the thermal efficiency of both receivers as illustrated in Figure 7, where the thermal efficiency is displayed during the day with a water flow rate of 7 L/h for both receiver tanks.

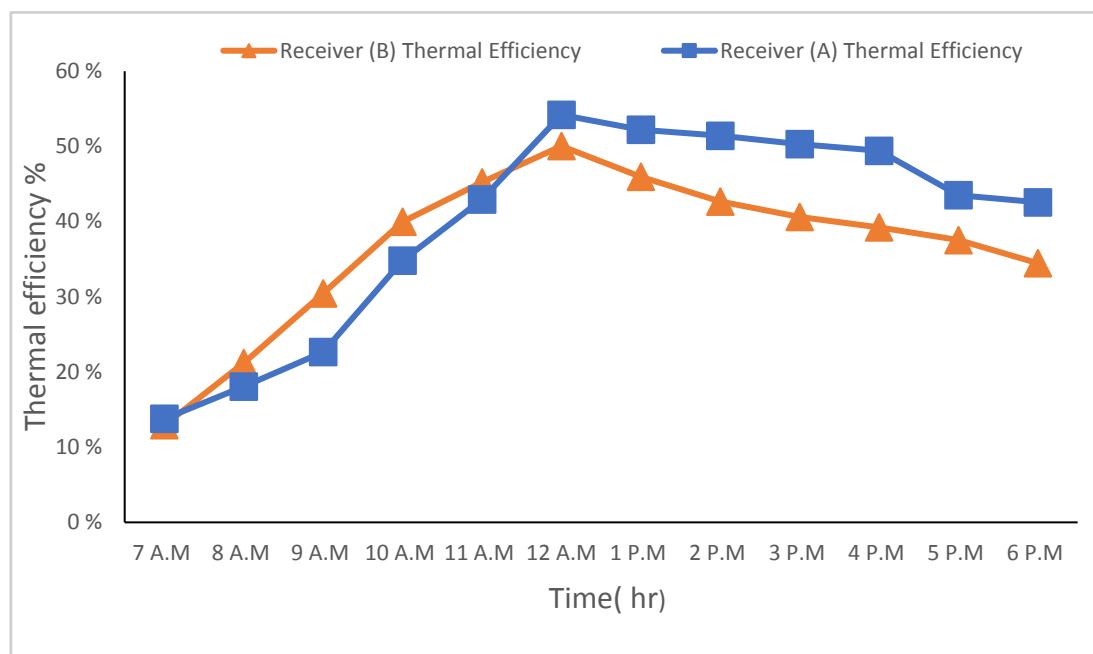


Figure 7. Variation of thermal efficiencies of receivers (A) and (B) with a flow rate of 7 L/hr.

It is inferred from Figure 7 that the receiver (B) hourly thermal efficiency amount is larger than that of the receiver (A) by more than (15%) before noon. However, receiver (A) thermal efficiency becomes considerably higher than that of (B) after 11:00 A.M. The thermal efficiency of receiver (A) becomes larger than that of the receiver (B) by about (8%) at noon and increases by about 20% in the afternoon. The paraffin wax used in receiver (A) provides a practical advantage over (B). Paraffin wax helped reduce the thermal losses in receiver (A), hence its thermal efficiency exceeded (B). In addition, results indicated that the daily efficiency of the receiver (A) on August 20, 2021, was 47.72%, whereas the daily efficiency of the receiver (B) was 40.64% on the same day.

4.2. Energy analysis of stage (2)—no flow rate

In the case where there was no water flow rate considered, different equations were used than those with flow rates for August 19 and 20 of 2021. Figure 8 presents the thermal energy stored in receivers (A) and (B).

It is inferred from Figure 8 that the thermal energy stored in the receiver tank (A) is considerably larger than that of the receiver tank (B) by about 11% at noon. The reason for this rise is the use of

paraffin wax. The thermal efficiency of both receivers reached a maximum value at noon. After noontime, the amount starts to decrease slightly until midnight. Before noon, the paraffin wax passes through a heating stage, at which it absorbs thermal energy from water. In addition, the experimental data are analyzed regarding the thermal efficiency of receivers (A) and (B), as indicated in Figure 9.

It is inferred from Figure 9 that the thermal efficiency hourly values of the receiver (A) exceed the hourly amounts of (B) by 10% at noon. They both start from 10% and increase until a maximum value of around 60% in the receiver (A), and roughly 55% in the receiver (B). Paraffin wax helped reduce the thermal losses in the receiver (A), hence its thermal efficiency exceeds (B). In addition, results indicated that the daily efficiency of the receiver (A) on August 20, 2021, was 41.59%, whereas the daily efficiency of the receiver (B) was 35.24% on the same day.

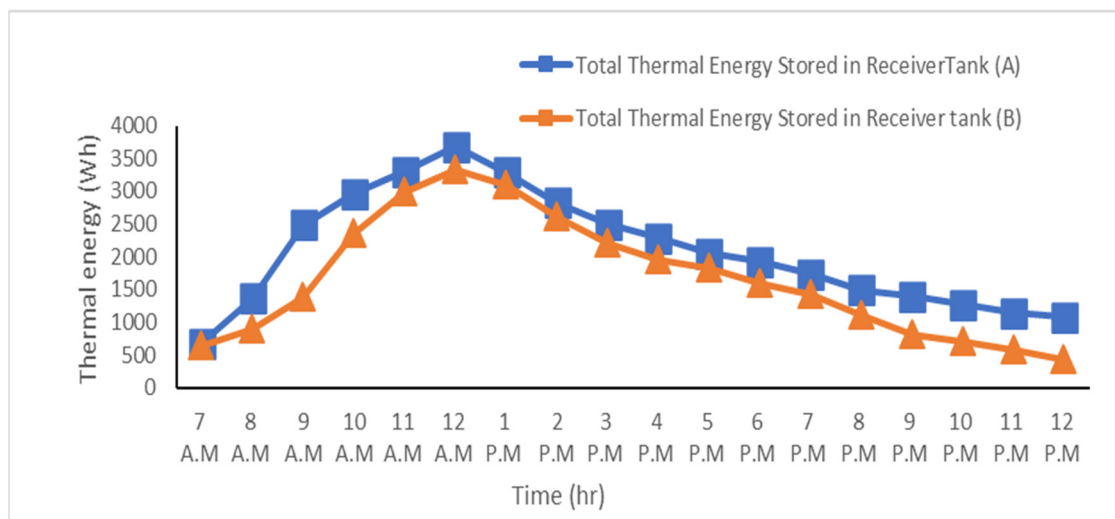


Figure 8. Variation of thermal energy stored in receivers (A) and (B) on August 21, 2021 with no water flow rate.

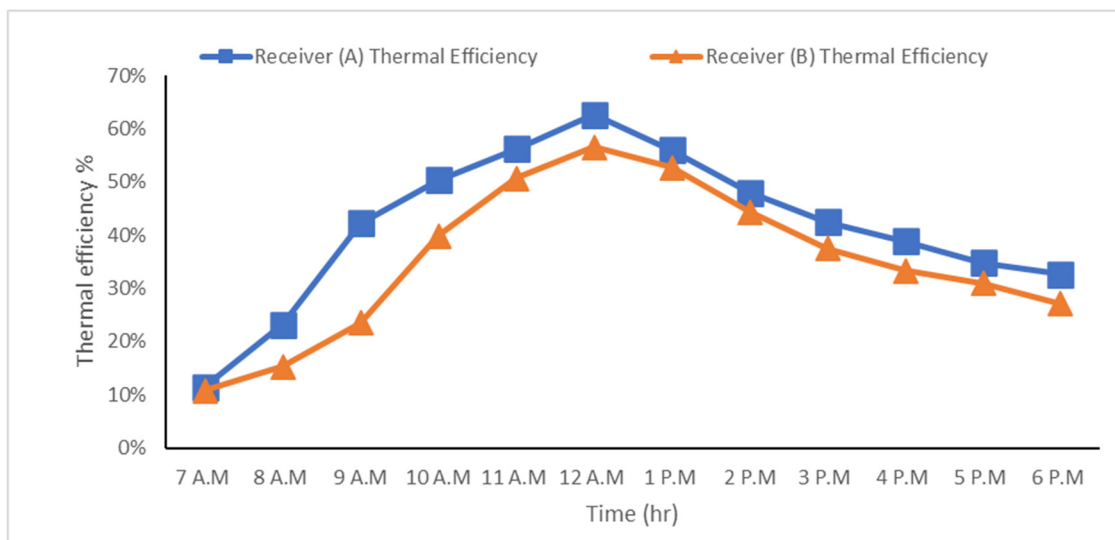


Figure 9. Variation of thermal efficiency stored in receivers (A) and (B) on August 21, 2021, with no flow rate.

4.3. Economic feasibility analysis results

Based on the calculations conducted using the equations presented in the mathematical modeling of this study. The economic feasibility of the solar evacuated tubes is compared to the electrical geyser. Table 3 presents the results of the comparison between the electrical geysers and solar evacuated tube water-in-glass collector, considering that the receiver (A) cost plus, the cost of paraffin wax is higher than the cost that (B).

Table 3. Results related to the comparison between the electrical geyser and solar water evacuated tube water-in-glass collector.

Category	Electric Geyser	Model (A) (with PCM)	Model (B) (with no PCM)
Initial capital cost	141 to 352 USD	423 to 704 USD	405.28 to 679 USD
Overall lifespan	7 to 12 years	10 to 15 years	10 to 15 years
Space requirement	Mounted on Wall	Needs a Roof for installation	Needs a roof for installation
Carbon emissions	Cause pollution due to combustion of coal and heavy fuel	Cause no pollution	Cause no pollution
Flexibility of installation	Easy	Easy	Easy
Source of power	Electricity	Solar radiation	Solar radiation

E_{HW} equals $(\dot{m}_w C p_w (T_{w,out} - T_{w,in}))$, or $(96 \text{ kg/day} \times 4.186 \times (70 - 20)) = 20100 \text{ kJ/day}$, considering $70 \text{ }^\circ\text{C}$ and $20 \text{ }^\circ\text{C}$ from the experimental procedure, are the average values of $T_{w,out}$, and $T_{w,in}$ along the year, respectively, and the \dot{m}_w is the water mass flow rate which is 7 L/h for 12 hours per days used in the experimental procedure. CE equals 16.44 USD cents/kWh [19]. η_{Coil} equals the efficiency of the electric geyser, which is 92% [20]. Substituting these values in Eq 11 leads to 269 USD/annum. In the Jordanian market the present worth (initial cost, IC) of the solar evacuated water-in-glass collector equals between 845 to 1,408 USD. Taking the average value of the present worth, 1,197 USD, then the $SV_{Solar-PCM}$ equals to 239 USD. The electric geyser salvage value, SV_{Geyser} , equals $211 \times (0.2) = 42.2 \text{ USD}$. The $O\&MC_{Solar-PCM}$ costs around 70.4 USD/annum depending on data from the Jordanian market. While the $O\&MC_{Geyser}$ equals 35 USD/annum based on the Jordanian market. Substituting all these values in Eq 10 leads to a solar-PCM annual system cost, $AC_{Sys-Solar-PCM}$, of 211 USD, while the electric geyser annual system cost, $AC_{Sys-Geyser}$ equals 327 USD. Figure 10 presents a comparison of annual cost and fuel cost between the solar thermal collector with paraffin wax with electric geyser. The annual fuel cost of a solar thermal collector is assumed as 7 USD (cost spent only for cleaning). The solar-PCM collector payback period (PBP) is calculated using Eq 15. The annual savings equal $(269) - (45) = 224 \text{ USD}$. Thus, $PBP = 1,197/224 = 5.35 \text{ years}$.

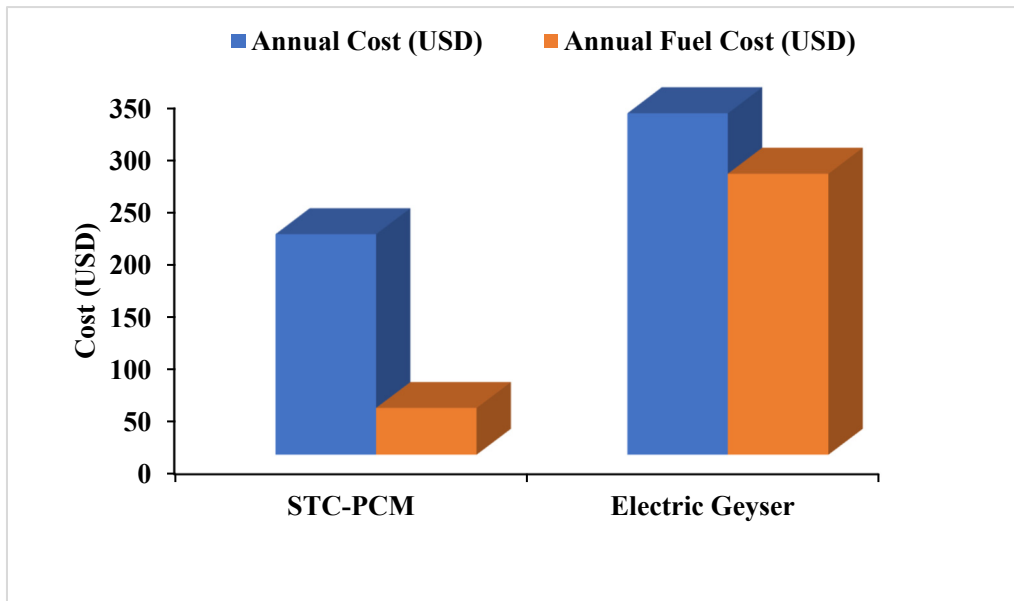


Figure 10. Comparison of annual cost and fuel cost between the solar thermal collector with paraffin wax with electric geyser.

4.4. Overall summary of the analysis results

The results related to the daily efficiency of receivers (A) and (B) for the two stages (7, and zero flow rates) are summarized in Figure 11.

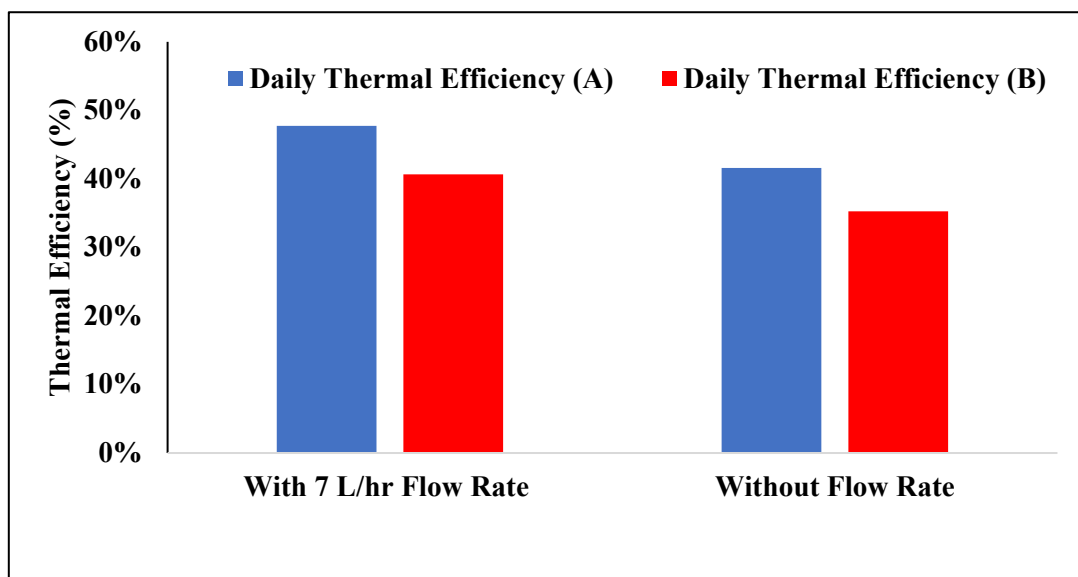


Figure 11. Comparison of daily thermal efficiencies with different flow rates.

It is inferred from Figure 11 that typically the thermal efficiency of receiver (A) is higher than that of (B) for all cases of flow rates. This can indicate a proof regarding the significant potential of paraffin wax integration to the solar thermal collector. This study investigates the performance and key significance of thermal storage for solar thermal systems, including water-in-glass evacuated tube

collector, via paraffin wax that is used to store the thermal energy for longer durations. The results revealed that the paraffin wax has valid testing results. It can be effectively used in several solar thermal systems to store thermal energy for longer periods. This result is consistent with the results of [7,15] who found that placing PCM (including paraffin and stearic acid) in the solar thermal system enabled a high quantity of thermal energy even when there is insufficient solar radiation during cold days. This result is also compatible with the results of [21] who found that using paraffin wax offered higher potential of thermal energy storage capacity to the system. This potential helped increase solar thermal collector efficiency and economic feasibility. This result is also consistent with the results of [10] who found that using PCM in this thermal system led to significant improvement in the storage potential of the solar collector. This result is also compatible with the results of [8] who found that using commercial-based paraffin in solar thermal systems is highly economically feasible. It enabled the extensions of the overall operating period of the solar thermal collector. Furthermore, the results of this research are consistent with the results of [16,17] who found that using PCM in evacuated tube systems can reduce the thermal energy losses and increase their thermal efficiency.

Table 4 presents a comparison of current results with those of a previous study made by K. Chopra et al. [18,21]. It can be noted that there is a good agreement between both results. It's also concluded that the optimal use of phase-changing materials with quality in solar thermal system increases the efficiency of the system, and from an economic point of view it is better than using electricity as it saves us a bill of high consumption of electrical energy, especially in periods of high hot water consumption.

Table 4. Comparison of present results of thermal efficiency, payback period and annual fuel cost with those of Chopra et al. [15].

	Present study		Previous study	
	Solar collector with PCM	Electric geyser	Solar collector with PCM	Electric geyser
Thermal efficiency %	47.72%	92%	40.92%	90%
Payback period	3.35 year	-	4.12 year	-
Annual fuel cost USD/Annum	211	269.76	226.18	264

5. Conclusions

This systematic study is conducted to investigate and assess the contribution and benefits of incorporating paraffin wax as a PCM into evacuated water-in-glass solar collector.

The main experimental conclusions of this study are:

1. The useful thermal energy stored in the receiver (A) with PCM is higher than that of receiver (B) without PCM by about 8.6% at noon and about 30% at early night. Whereas, the solar evacuated tube water-in-glass thermal collectors integrated with PCM can improve the solar collector's thermal efficiency by roughly (7%).
2. Using a flow rate of 7 L/hr, the receiver (A) daily thermal efficiency is 47.72%. Whereas the receiver (B) daily thermal efficiency is 40.64%. The thermal efficiency of the receiver (A) is larger than the receiver (B) by about (8%) at noon, and increases by about 20% in the afternoon.
3. With no water flow rate, receiver (A) daily thermal efficiency is 41.59%. Whereas the receiver (B) daily thermal efficiency is 35.24%. The thermal efficiency of receiver (A) is larger than that of

receiver (B) by about (10%) at noon.

4. The solar thermal collector (A) annual cost is around 211 USD/annum. Whilst its annual fuel cost is estimated as 45 USD. In comparison, the annual cost of a geyser is 327 USD/annum. Whilst the geyser's annual fuel cost is 269 USD.
5. The payback period of the solar thermal collector (A) with PCM is estimated as 5.35 years.
6. Depending on the findings obtained from the experimental analysis of models (A) and (B), the authors recommend some aspects for future work that can improve the results of the experimental analysis conducted in this study, including the change in the quantity of paraffin wax for observing the optimum charge of PCM that would provide maximum thermal efficiency increase.

Acknowledgments

My thanks and appreciation also to Prof. Dr. Hendry Ammari Department of Mechanical Engineering at Mutah University, for supporting me and providing me with greater assistance, through his worthwhile comments as I work on my thesis.

Thanks, and appreciation to all the faculty members of the Engineering Department at Mutah University, as many of them guided me during the investigation of my thesis.

Conflict of interest

The authors declare no conflict of interest.

Author contributions

Conception and design of study: Akthem Mohi Al-Abdali, Handri Ammari.

Drafting the manuscript: Akthem Mohi Al-Abdali.

Analysis and/or interpretation of data: Handri Ammari.

References

1. Ghosh SK (2020) Fossil fuel consumption trend and global warming scenario: Energy overview. *Glob J Eng Sci*, 5. <https://doi.org/10.33552/gjes.2020.05.000606>
2. Saini V, Tripathi R, Tiwari GN, et al. (2018) Electrical and thermal energy assessment of series connected N partially covered photovoltaic thermal (PVT)-compound parabolic concentrator (CPC) collector for different solar cell materials. *Appl Therm Eng* 128: 1611–1623. <https://doi.org/10.1016/j.applthermaleng.2017.09.119>
3. Shamshirgaran SR, Al-Kayiem HH, Sharma K, et al. (2020) State of the art of techno-economics of nanofluid-laden flat-plate solar collectors for sustainable accomplishment. *Sustainability*, 12. <https://doi.org/10.3390/su12219119>
4. Abd-Elhady MS, Nasreldin M, Elsheikh MN (2018) Improving the performance of evacuated tube heat pipe collectors using oil and foamed metals. *Ain Shams Eng J* 9: 2683–2689. <https://doi.org/10.1016/j.asej.2017.10.001>

5. Venkatacha C, Mariam SG, Chimdo Anc A (2018) Thermal and economic analysis review on flat plate, parabolic trough and evacuated tube solar collectors for process heat applications. *J Appl Sci* 19: 1–8. <https://doi.org/10.3923/jas.2019.1.8>
6. Benchara EH, Jennah S, Belouggadia N, et al. (2020) Thermal energy storage by phase change materials suitable for solar water heaters: An updated review. In: *2020 IEEE 2nd International Conference on Electronics, Control, Optimization and Computer Science, ICECOCS 2020*: 1–10. <https://doi.org/10.1109/ICECOCS50124.2020.9314561>
7. Reddy RM, Nallusamy N, Hariprasad T (2012) Solar energy based thermal energy storage system using phase change materials. *Int J Renewable Energy Technol* 3: 11–23. <https://doi.org/10.1504/ijret.2012.043905>
8. Lin W, Ma Z, Ren H (2020) Solar thermal energy storage using paraffins as phase change materials for air conditioning in the built environment. In: *Paraffin—an Overview*. <https://doi.org/10.5772/intechopen.86025>
9. Sadeghi G, Pisello AL, Nazari S (2021) Empirical data-driven multi-layer perceptron and radial basis function techniques in predicting the performance of nanofluid-based modified tubular solar collectors. *J Clean Prod* 295: 126409. <https://doi.org/10.1016/j.jclepro.2021.126409>
10. Yeh CY, Boonk KJF, Sadeghi G, et al. (2022) Experimental and numerical analysis of thermal performance of shape stabilized PCM in a solar thermal collector. *Case Stud Therm Eng* 30: 101706. <https://doi.org/10.1016/j.csite.2021.101706>
11. Shoeibi S, Kargarsharifabad H, Mirjalily SAA, et al. (2022) A comprehensive review of nano-enhanced phase change materials on solar energy applications. *J Energy Storage* 50: 104262. <https://doi.org/10.1016/j.est.2022.104262>
12. Hussein HA, Abed AH, Abdulmunem AR (2016) An experimental investigation of using aluminum foam matrix integrated with paraffin wax as a thermal storage material in a solar heater. *Proceeding of the 2nd Sustainable & Renewable Energy Conference, Baghdad-Iraq*, 26–27. Available from: https://www.academia.edu/35718536/An_experimental_investigation_of_using_aluminum_foam_matrix_integrated_with_paraffin_wax_as_a_thermal_storage_material_in_a_solar_heater.
13. Regin AF, Solanki SC, Saini JS (2006) Latent heat thermal energy storage using cylindrical capsule: Numerical and experimental investigations. *Renewable Energy* 31: 2025–2041. <https://doi.org/10.1016/j.renene.2005.10.011>
14. Manoj Kumar P, Myslamsy K (2019) Experimental investigation of solar water heater integrated with a nanocomposite phase change material: Energetic and exergetic approach. *J Therm Anal Calorim* 136: 121–132. <https://doi.org/10.1007/s10973-018-7937-9>
15. Chopra K, Tyagi V, Pathak AK (2019) Experimental performance evaluation of a novel designed phase change material integrated manifold heat pipe evacuated tube solar collector system. *Energy Convers Manag* 198: 111896. <https://doi.org/10.1016/j.enconman.2019.111896>
16. Carnevale E, Lombardi L, Zanchi L (2014) Life cycle assessment of solar energy systems: Comparison of photovoltaic and water thermal heater at domestic scale. *Energy* 77: 434–446. <https://doi.org/10.1016/j.energy.2014.09.028>
17. Ameen M, Xiaochan W, Yaseen M, et al. (2018) Performance evaluation of root zone heating system developed with sustainable materials for application in low temperatures. *Sustainability* 10: 4130. <https://doi.org/10.3390/su10114130>

18. Algarni S, Mellouli S, Alqahtani T (2020) Experimental investigation of an evacuated tube solar collector incorporating nano-enhanced PCM as a thermal booster. *Appl Therm Eng* 180: 115831. <https://doi.org/10.1016/j.applthermaleng.2020.115831>
19. Betancourt ROJ, López JMG, Espejo EB, et al. (2020) Iot-based electricity bill for domestic applications. *Sensors* 20: 6178. <https://doi.org/10.3390/s20216178>
20. Tangwe S, Simon M, Meyer E (2015) Quantifying residential hot water production savings by retrofitting geysers with air source heat pumps. In: *Proceedings of the 23rd Conference on the Domestic Use of Energy, DUE 2015*, 235–241. <https://doi.org/10.1109/DUE.2015.7102986>
21. Evangelisti L, de Lieto Vollaro R, Asdrubali F (2019) Latest advances on solar thermal collectors: A comprehensive review. *Renewable Sustainable Energy Rev* 114: 109318. <https://doi.org/10.1016/j.rser.2019.109318>



AIMS Press

© 2022 the Author(s), licensee AIMS Press. This is an open access article distributed under the terms of the Creative Commons Attribution License (<http://creativecommons.org/licenses/by/4.0>)